Poster 03-08 : 25 Years of Science with Chandra Symposium : Boston MA : 2024 Dec 3

Persistence of Quiescence on active dMe star EV Lac

Vinay L. Kashyap (CfA), Robert Zimmerman (Imperial/Toronto), David van Dyk (Imperial), Aneta Siemiginowska (CfA)

CONTEXT: We have analyzed the long duration Chandra ACIS-S/HETG datasets of active flaring dMe star EV Lac to separate the light curve into instances of flaring and quiescence. We use a Hidden Markov Model formulation (*Zimmerman et al. 2024 MNRAS*; see also poster 03-06 by *R.Zimmerman here*) applied to a set of low- and high-energy passband light curves (see **Figure 1 top**) to define instantaneous states based on the spectral hardness information (**Figure 1 middle**), which are then separated into two clusters to represent flaring and quiescence (**Figure 1 bottom**). We confirm through spectral fitting (see **Table**) that the quiescent and flaring durations thus separated are well distinguished in their thermal properties. The individual flares have a broad scatter in their spectral hardnesss, and are always harder than the quiescent state (**Figure 2**),

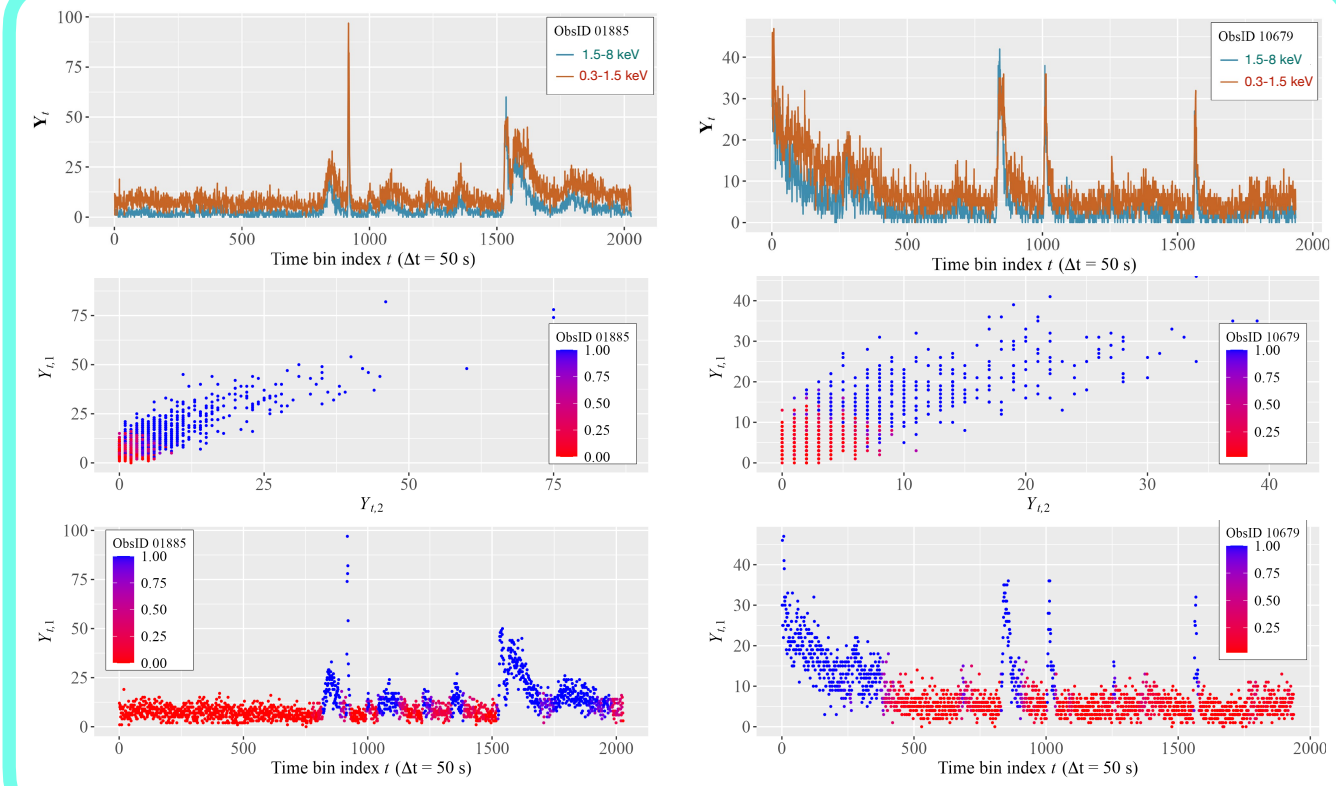

FIGURE 1: [TOP] Light curves of EV Lac in 50 s bins in low-energy (0.3-1.5 keV) and high-energy (1.5-8 keV) bands
[MIDDLE] Hidden Markov states color coded according to 2nd stage classification
[BOTTOM] Lower-energy band light curve with quiescent/flaring classification marked.

CONCLUSIONS: We find a remarkable constancy in the properties of the quiescent spectra between the two observations separated by ≈8 years (**Figures 2&3**). The temperatures, emission measures, and abundances during quiescence are all consistent across the epochs, suggesting that a steady heating mechanism is operating on the star. This is consistent with several recent studies finding similar instances of a steady non-varying component to the heating in active stars (e.g., YZ Cmi [Raasen et al. 2007], AR Lac [Drake et al. 2014], XZ Tau [Silverberg et al. 2023]). Flaring intervals 30-40% of the time, contribute ≈60% of the observed counts, and individual flare properties vary widely (see also Huenemoerder et al. 2010).

ObsID	Obs Date	Exposure	kT_{LOW} [keV]	EM_{LOW} [$\times 10^{10}$ cm^{-3}]	kT_{HIGH} [keV]	EM_{HIGH} [$\times 10^{10}$ cm^{-3}]	$Z_\odot$	Number Flares	Flaring Time	21:23Å/19Å ≡ O7/O8	12Å/19Å ≡ Ne10/O8	19Å/(15,17)Å ≡ O8/Fe17
1885	Sep 2001	100 ksec	0.35 ±0.0024	1.6±0.04	1.26 ±0.007	0.99±0.01	0.17	15	40%	1.16±0.11 Q 1.32±0.12 F	0.28±0.02 Q 0.46±0.03 F	1.51±0.10 Q 1.27±0.09 F
10679	Mar 2009	96 ksec	0.35 ±0.003	1.5±0.05	1.35 ±0.009	0.95±0.01	0.17	11	30%	1.14±0.13 Q 1.06±0.14 F	0.30±0.02 Q 0.40±0.03 F	1.78±0.14 Q 1.74±0.15 F

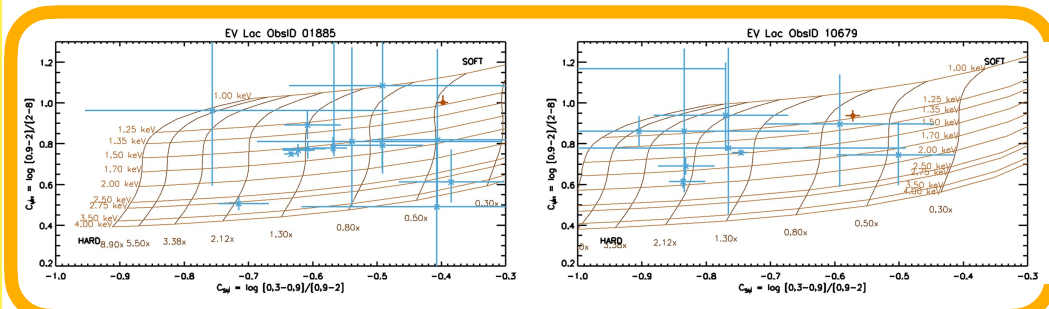

FIGURE 2: Color-color (Soft-Medium vs Medium-Hard) scatterplot for the combined quiescent (red point) and each of the flaring (blue points) intervals. The grid defines a 2-T thermal model with kT_{LOW} fixed at 0.35 keV, and with varying kT_{HIGH} and EM_{HIGH}/EM_{LOW}. The grid includes corrections for ACIS effective area. The quiescent plasma is consistent with a 2-T plasma with $EM_{HIGH} \approx 0.5 \cdot EM_{LOW}$ and kT_{HIGH}=1.25 keV.

Zimmerman+2024

MNRAS 534, 2142

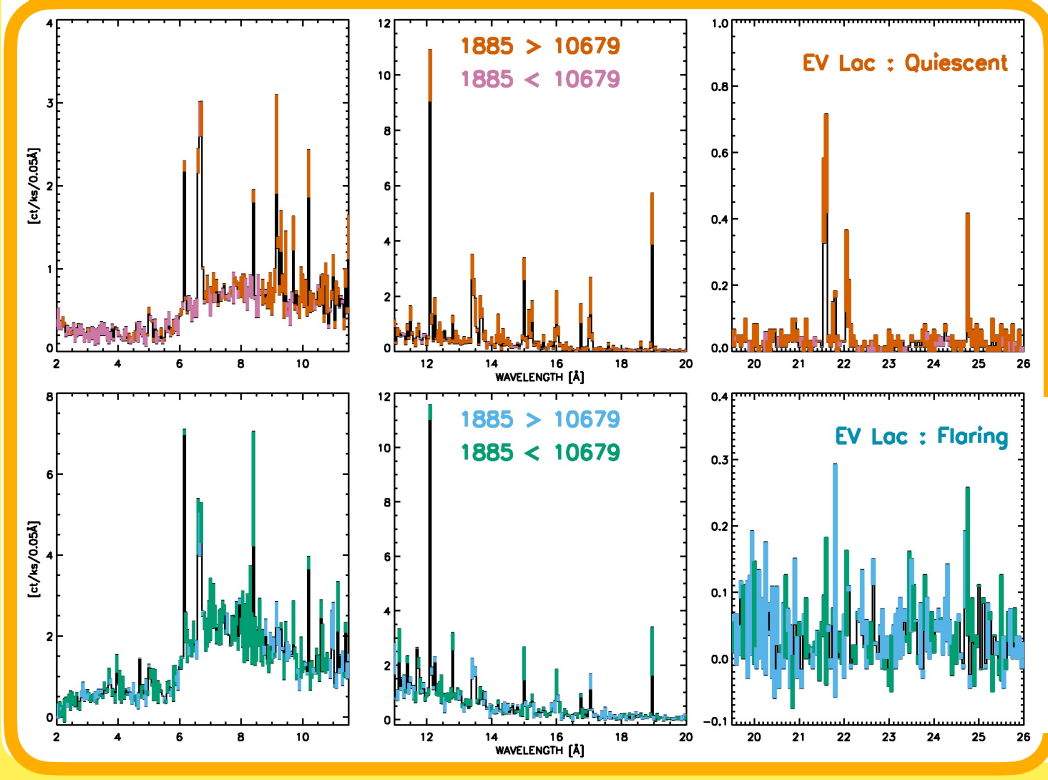

FIGURE 3: Comparing the EV Lac HEG+MEG count rate spectra between different epochs for the quiescent **[TOP]** and flaring **[BOTTOM]** intervals. The flaring spectra have had the quiescent component subtracted out. The three **columns** are split into different wavelength ranges for the sake of visibility of line emission structure. Spectral bins where one or the other epoch has more counts are marked with shadings as denoted in the middle panels. Notice that the differences during quiescence are small, even in prominent lines except at λ>15 Å (e.g., **right column**), where the later epoch always has a lower count rate because of contamination buildup in ACIS.

Generalized Hidden Markov Model to describe light curves in two passbands. See poster 03-06 (*Zimmerman et al.*, this Symposium) for details.

In the adopted model shown in **Figure 1**, ρ=1 and ϕ_1=ϕ_2.

$$\mathbf{Y}_t \mid \mathbf{X}_t \sim \text{Poisson}(w \cdot \beta_1 \cdot e^{X_{t,1}}) \cdot \text{Poisson}(w \cdot \beta_2 \cdot e^{X_{t,2}}).$$

$$\mathbf{X}_t = \mathbf{\Phi}\mathbf{X}_{t-1} + \boldsymbol{\varepsilon}_t,$$

$$\mathbf{\Phi} = \begin{bmatrix} \phi_1 & 0 \\ 0 & \phi_2 \end{bmatrix},$$

$$\boldsymbol{\varepsilon}_t \overset{\text{iid}}{\sim} \mathcal{N}_2(\mathbf{0}, \mathbf{\Sigma}), \text{ and}$$

$$\mathbf{\Sigma} = \begin{bmatrix} \sigma_1^2 & \sigma_1\sigma_2\rho \\ \sigma_1\sigma_2\rho & \sigma_2^2 \end{bmatrix}.$$

$\mathbf{Y}_t$ are counts at time t

$\mathbf{X}_t$ are HMM states

[12] are passbands

w is a normalizing scaling factor

$\mathbf{\Sigma}$, $\mathbf{\Phi}$, and $\beta_{[12]}$ are fit parameters